Effect of Diffusion Stopper Layer on Surface Morphology of MgO Underlayer of $L1_0$-FePt Granular layer for HAMR

Daiki Isurugi, Feng Chenming, Akihiro Shimizu, Shintaro Hinata, Tomoyuki Ogawa, and Shin Saito

Department of Electronic Engineering, Graduate School of Engineering, Tohoku University,
6–6–05, Aoba, Aramaki, Aoba–ku, Sendai 980–8579, Japan, daiki.isurugi.a1@tohoku.ac.jp

Due to the highly oriented (001) sheet texture of $L1_0$-FePt grains in HAMR media, a heteroepitaxial sputtered multilayer consisting of amorphous alloy/ (001)-bcc alloy/ (001)-fcc MgO is used as the underlayer. However diffusion of the amorphous elements into the grain boundaries of the bcc layer causes nucleation of the bcc grains with preferred orientation of (110) plane, which brings nodule-like abnormal growth of MgO with (111) sheet texture. In this study, we investigated the effect of inserting a diffusion stopper layer (DSL) to prevent the forming of nodules, and found that by thickening a 0- 5 nm DSL, nodule density was reduced 200/μm^2 to 28/μm^2 while maintaining the MgO underlayer with (002) sheet texture.

***Index Terms*— Magnetic recording, HAMR, $L1_0$–FePt, MgO**

I. Introduction

As traditional perpendicular magnetic recording faces limitations in achieving higher areal densities, HAMR leverages localized laser heating to reduce coercivity in the recording layer, enabling efficient data writing [1]. The media structure is consisted of amorphous/ (001)bcc-alloy/ (001)fcc-MgO/ $L1_0$-FePt granular layer is used as the underlayer. However, critical challenges persist in material and structural control. Key issues include the formation of nodular structures on the MgO underlayer surface, caused by diffusion of amorphous-layer elements constituents from grain boundaries during deposition [2- 6]. In this study, we investigated the effect of inserting a diffusion stopper layer to prevent diffusion of the elements constituting the amorphous layer into the bcc layer.

II. Results and Discussion

A. *Mechanism of forming nodule structure [2]*

The mechanism of forming nodule structure was confirmed. Fig. 1 shows the AFM topography image of the MgO(5) / CrMn(30) / CoW(50) film with area of 500 x 500 nm square when CrMn layer was deposited at 305 °C. It can be confirmed that there are two characteristic surface structures. One is a network-shaped upheaval structure with a height of 2 nm, a width of 10 nm and an interval of 30 nm observed throughout the sample, and the other is a nodule structure with a height of 3 nm and a width of several tens nm. This study focused on the nodule structure.

In order to investigate the formation factor of the nodule structure, a structural analysis in the direction of the film thickness near the structure was carried out using cross-sectional TEM analysis. Fig. 2 shows cross-sectional BF-STEM image around the nodule for a MgO(5) / CrMn(30) / $Co_{60}W_{40}$ film. The CrMn grain has a nodule structure at the lower part of the site where the nodule structure of the MgO layer surface was observed. Lattice spacing of the surrounding CrMn layer were investigated and it was found that the film surface and the (110) plane were parallel to each other at the nodule forming portion and the (002) plane was parallel at portions where there are no nodules. Figure 3 (a) shows the STEM-HAADF image of the same field of view, and (b), (c), and (d) show the EDX mapping images by the characteristic X-rays of Co, Cr and Mn, respectively. According to the HAADF image, a white contrast portion in the CrMn layer is observed in a stripe shape in the film thickness direction avoiding the nodule structure. According to the EDX image, it can be seen that existence of Co corresponds to the white portion of the HAADF image. From the above results, it was found that the nodule portion on the surface of the MgO layer corresponds to the (110) oriented CrMn grain which is different orientation from the other portion in the CrMn layer, and it is suggested that the nodule is due to the (110) oriented CrMn grain generated at the grain boundary of (002) oriented CrMn grains in the growth process. The reason for the surface roughness is presumed to be caused by different growth rate of the CrMn according to the crystal orientation.

Finally, from the above results, we consider the formation origin of nodule structure. When the amorphous elements and Mn diffuse from the grain boundary of CrMn layer, in some of grain boundaries, (110) oriented CrMn grains which have different crystal orientations are generated in the upper layer of the CrMn layer, and a nodule structure is formed on the surface of the CrMn layer. It is considered that MgO layer grow so as to cover this portion, and a nodule structure is formed on the surface of the MgO layer.

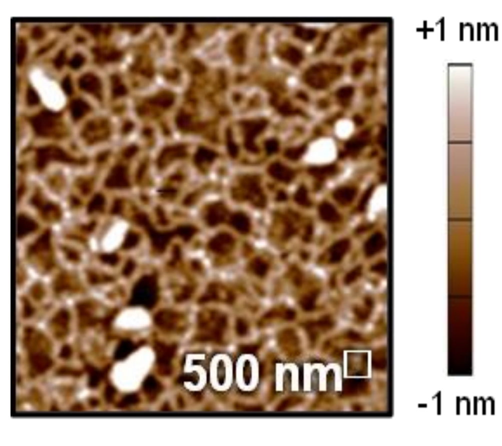

Fig. 1 AFM topography image of a MgO/ CrMn/ $Co_{60}W_{40}$ film at T_{sub}^{CrMn} of 305 °C.

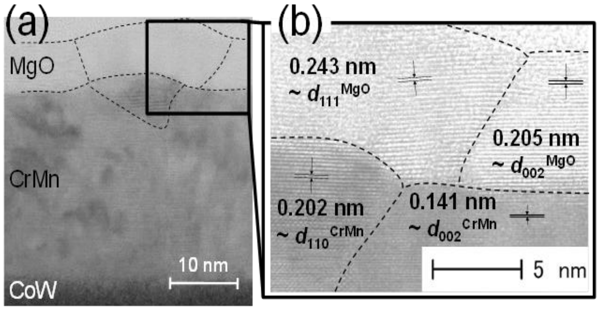

Fig. 2 Cross sectional BF-STEM image around nodule structure for a MgO/ CrMn/ $Co_{60}W_{40}$ film at T_{sub}^{CrMn} of 305 °C.

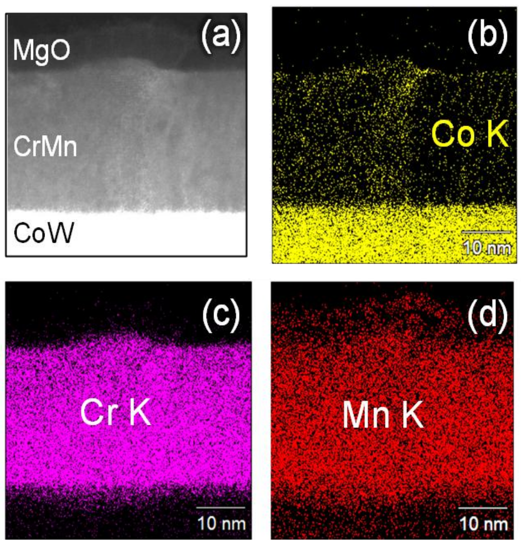

Fig. 3 (a) Cross sectional STEM-HAADF image and (b), (c), (d) -EDX maps of Co, Cr, and Mn around nodule structure for a MgO/ CrMn/ $Co_{60}W_{40}$ film at T_{sub}^{CrMn} of 305 °C.

B. Effect of inserting a diffusion stopper layer

Based on the consideration of the previous chapter, the dependence of the nodule occurrence number on MgO diffusion stopper layer (DSL) thickness was investigated. This chapter investigates strategies to enhance the crystal orientation and surface morphology of MgO thin films heteroepitaxially grown on orientation control layer (OCL) with diffusion stopper layer (DSL), aiming to optimize the FePt granular recording layer in Heat-Assisted Magnetic Recording (HAMR) media. Fig. 4 shows the stacking structure used in this experiment. As the DSL, MgO was deposited in a thickness of 1-5 nm.

Figure 5 shows AFM images of MgO surface structure and relationship between nodule density and DSL thickness. It shows even a 1 nm MgO DSL significantly suppresses nodule formation. By integrating a 0- 5 nm DSL, nodule density was reduced 200/μm^2 to 28/μm^2. From the above, it can be considered that the MgO diffusion stopper layer decreases the diffusion of amorphous constituent elements.

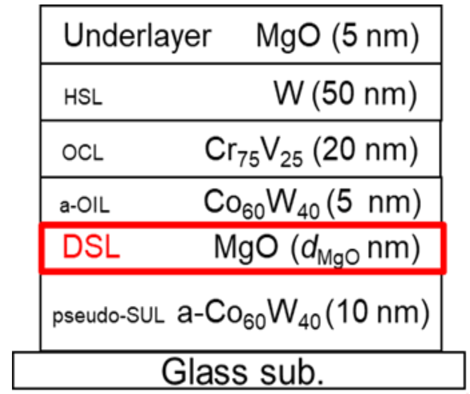

Fig. 4 The stacking structure used in this experiment.

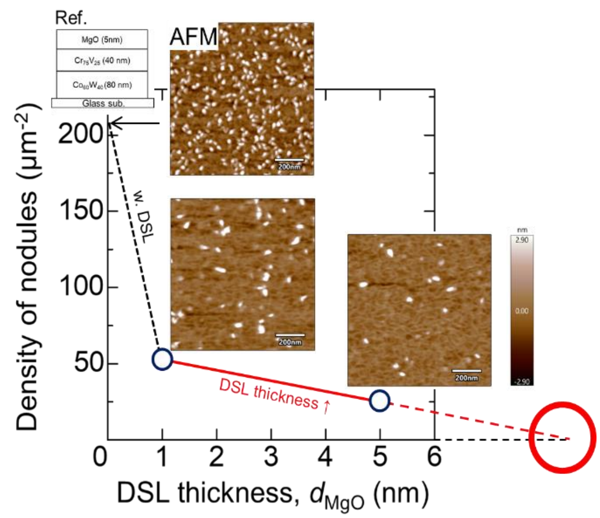

Fig. 5 AFM images of MgO surface structure and relationship between nodule density and DSL thickness.

References

[1] A. Chernyshov, T Le, B. Livshitz, O. Mryasov, C. Miller, R. Acharya, D. Treves, "Measurement of Curie temperature distribution relevant to heat assisted magnetic recording," *J. Appl. Phys.*, **117**, 17D111 (2015).

[2] A. Shimizu, S-J. Jeon, S. Hinata, S. Jo, and S. Saito, "The Network-Shaped Upheaval Structure in (002) Textured MgO layer for $L1_0$ FePt-Based Granular Media with Columnar Nanostructure", *IEEE Trans. Magn.*, **55**, 3200208 (2019).

[3] A. Shimizu, S. Hinata, S. Jo, and S. Saito, "Proposal of network-shaped upheaval structure using grain boundary diffusion in underlayer for $L1_0$ FePt-based granular media with columnar nanostructure", *T. Magn. Soc. Jpn.* (Special Issues), **3**, 7 (2019).

[4] S. Hinata, S. Jo, and S. Saito, „"Surface structure of MgO underlayer with Ti diffusion for (002) oriented $L1_0$ FePt based heat assisted magnetic recording media", *AIP Adv.,* **8**, 056515 (2018).

[5] S-J. Jeon, S. Hinata, and S. Saito, "Amorphous Cr-Ti Texture-inducing Layer Underlying (002) Textured bcc-Cr alloy Seed Layer for FePt-C based Heat-assisted Magnetic Recording Media", *J. Magn. Soc.* **21**, 35 (2016).

[6] S-J. Jeon, S. Hinata, S. Saito and M. Takahashi, "Highly (002) textured large grain bcc $Cr_{80}Mn_{20}$ seed layer on $Cr_{50}Ti_{50}$ amorphous layer for FePt-C granular film", *J. Appl. Phys.*, **117**, 17A924 (2015).